

Dependence of the Gamma-Ray Emission from SN 1006 on the Astronomical Parameters

L.T. Ksenofontov^a, E.G. Berezhko^a, H.J. Völk^b, V.K. Yelshin^a

(a) *Yu.G. Shafer Institute of Cosmophysical Research and Aeronomy, 31 Lenin Ave., 677980 Yakutsk, Russia*

(b) *Max-Planck-Institut für Kernphysik, Postfach 103980, D-69029, Heidelberg, Germany*

Presenter: L.T. Ksenofontov(ksenofon@ikfia.ysn.ru), rus-ksenofonov-L-abs2-og22-oral

We use nonlinear kinetic theory to study cosmic ray acceleration and the properties of the nonthermal emission from the supernova remnant SN 1006. The known range of astronomical parameters is examined in order to find out whether it encompasses the existing synchrotron emission data. It is shown that the hadronic gamma-ray flux is very sensitive to the ambient gas density N_H and that the existing H.E.S.S. upper limit requires $N_H < 0.1 \text{ cm}^{-3}$. The amplified magnetic field downstream of the shock amounts to about $150 \mu\text{G}$.

1. Introduction

The supernova remnant (SNR) SN 1006, located at the distance $d \approx 2 \text{ kpc}$, has been extensively observed throughout the electromagnetic spectrum. Observations of nonthermal X-rays [1] suggest that at least CR electrons are accelerated in SN 1006 up to energies of about 100 TeV. Subsequent γ -ray observations with the CANGAROO telescopes [2] strengthened this conclusion. It was also shown [3] that nonlinear kinetic theory of CR acceleration is consistent with all observational data for a value $N_H = 0.3 \text{ cm}^{-3}$ of the ambient interstellar medium (ISM) density from the range $0.05 \leq N_H \leq 0.3 \text{ cm}^{-3}$ existing in the literature. However, SN 1006 could not be detected by the H.E.S.S. experiment as a TeV source in a total of 18.2h (in 2003) and 6.3h (in 2004) livetime of ON source observations with SN 1006 in the field of view [4]. The H.E.S.S. upper limit is roughly one order of magnitude lower than the published CANGAROO flux.

As in our early study [3] we apply here nonlinear kinetic theory of CR acceleration in SNRs [5, 6] to find the optimum set of physical parameters of SN 1006, mainly the external parameter N_H , which give a consistent description of the observed overall dynamics and of the nonthermal emission.

2. Results and discussion

Since SN 1006 is a type Ia supernova it presumably expands into a uniform ISM, ejecting roughly a Chandrasekhar mass $M_{ej} = 1.4M_\odot$, which is characterized by the initial velocity distribution $dM_{ej}/dv \propto v^{2-k}$ with $k = 7$. Since the SNR is already in the Sedov phase, its properties are not sensitive to the parameters values M_{ej} and k of the ejecta. The ISM gas density $\rho_0 = 1.4m_p N_H$, which is usually characterized by the hydrogen number density N_H , is an important parameter which strongly influences the expected SNR dynamics and nonthermal emission. However, the value of N_H is poorly constrained for SN 1006 from the thermal emission observations. They yield a wide range of possible values from $N_H = 0.05 - 0.1 \text{ cm}^{-3}$ [7] to $N_H \approx 0.3 \text{ cm}^{-3}$ [8].

We shall take as the most reliable estimate for the distance $d = 2.2 \text{ kpc}$ to SN 1006 [9].

In Fig. 1 we present the time dependence of the shock radius R_s and of the shock speed V_s , calculated for the optimum upstream magnetic field value $B_0 = 30 \mu\text{G}$, and for the expected density range of the ambient ISM. The value of the explosion energy was taken to fit the observed size and speed at the current epoch $t \approx 10^3 \text{ yr}$. Since SN 1006 has already evolved into the Sedov phase, the explosion energy scales as $E_{sn} \propto N_H$.

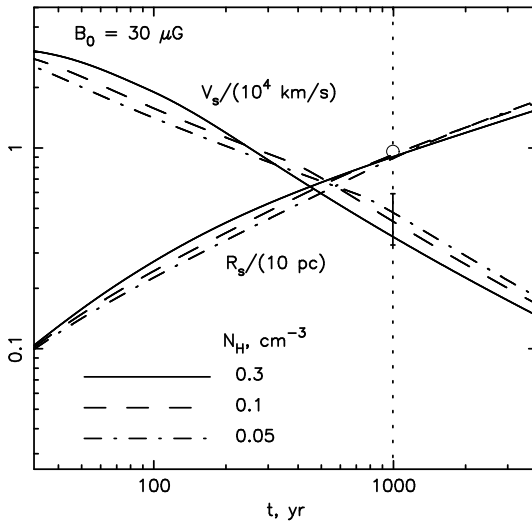


Figure 1. Shock radius R_s and shock speed V_s as a function of time for the upstream magnetic field $B_0 = 30 \mu\text{G}$ and different ISM number densities N_H . The observed size and speed of the shock [10], are shown as well.

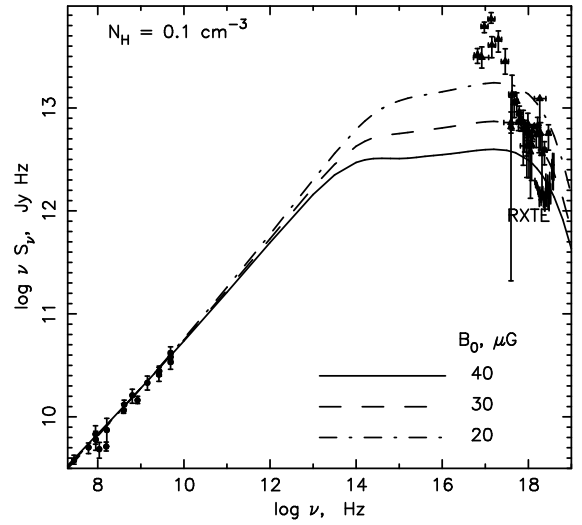


Figure 2. Synchrotron emission flux as a function of frequency for the ISM number density $N_H = 0.1 \text{ cm}^{-3}$ and different upstream magnetic fields. The observed X-ray [11, 12] and radio emission [13] fluxes are shown.

The calculations correspond to $E_{sn}/(10^{51} \text{ erg}) = 1.9, 3.8$ and 11.4 , for $N_H/(1 \text{ cm}^{-3}) = 0.05, 0.1$ and 0.3 , respectively. The calculations shown in Fig. 1 demonstrate that with this dependence of E_{sn} on N_H the SNR dynamics is indeed compatible with the measured values of $R_s(t)$ and $V_s(t)$ for different ISM densities.

In our model the interior (downstream) magnetic field B_d is connected with the outer (upstream) magnetic field B_0 by the simple relation $B_d = \sigma B_0$, where σ is the overall shock compression ratio [3]. It is also assumed that already the upstream field B_0 is significantly amplified as a consequence of CR streaming, and that it therefore exceeds the existing ISM value substantially [14]. The shock compression ratio depends on the ambient gas density. For the case $B_0 = 30 \mu\text{G}$ used in Fig. 1, the downstream magnetic field strengths are $B_d = 149, 156$, and $173 \mu\text{G}$ for $N_H = 0.05, 0.1$, and 0.3 cm^{-3} , respectively.

For the global determination of the effective downstream field B_d we compare the theoretical synchrotron spectrum, calculated for three different values of B_0 , with the observed spatially integrated spectrum (see Fig. 2). In order to reproduce the radio spectral index $\alpha = 0.57$, observed for SN 1006, one needs efficient CR acceleration with a proton injection rate $\eta = 2 \times 10^{-4}$, which leads to the required shock modification. To fit the amplitude of radio flux we take the electron to proton ratio $K_{ep} = 2.6 \times 10^{-3}, 1.1 \times 10^{-3}$ and 4.2×10^{-4} for $N_H = 0.05, 0.1$ and 0.3 cm^{-3} respectively.

X-ray synchrotron spectral measurements are required to find the optimum value of the magnetic field strength B_d [3, 15]: for a given fit of the synchrotron spectrum in the radio range the X-ray synchrotron amplitude is very sensitive to B_d (see Fig. 2). An increase of the magnetic field B_d leads to a decrease of the electron energy $\epsilon_l \propto t^{-1} B_d^{-2}$ [3], where the electron spectrum undergoes a brake: for $\epsilon > \epsilon_l$ synchrotron losses in the downstream region are significant and lead to a steep overall (spatially integrated) electron spectrum $N_e \propto \epsilon^{-\gamma-1}$, where γ is the power law index of the CR spectrum at the shock front. Therefore the synchrotron spectrum has a break at the corresponding frequency $\nu_l \propto \epsilon_l^2 B_d \propto B_d^{-3}$, which decreases with increasing B_d , as one can see in Fig. 2.

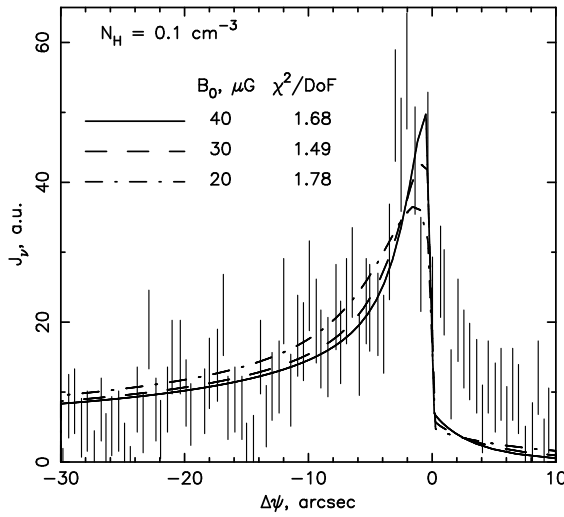


Figure 3. Projected radial dependence of the non-thermal X-ray brightness in the energy range 2 to 10 keV, calculated for the same cases as in Fig. 2 together with the Chandra data corresponding to the sharpest profile in [16].

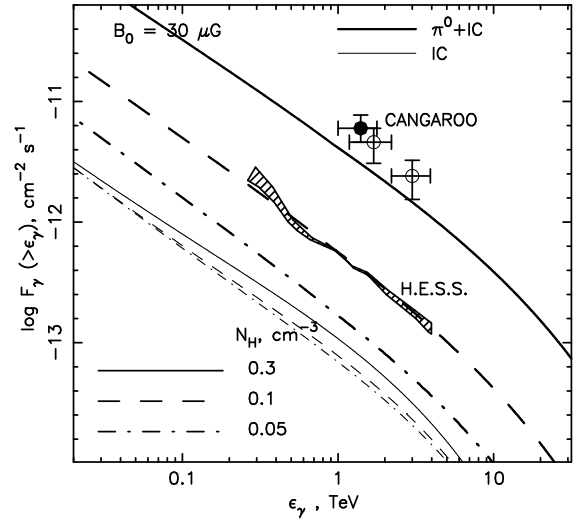


Figure 4. Total (π^0 -decay + IC) (*thick lines*) and IC (*thin lines*) integral γ -ray energy fluxes from the NE half of the remnant as a function of γ -ray energy for the same cases as in Fig. 1. The CANGAROO flux from the NE rim [20] and the corresponding H.E.S.S. upper limit for the CANGAROO position [4] are shown as well.

We now compare this globally determined magnetic field value $B_0 = 30 \mu\text{G}$ with the local Chandra results by plotting the full numerical solutions for the overall SNR morphology jointly with the sharpest of the experimental brightness profile of the nonthermal X-ray emission obtained by the Chandra observers [16] in Fig. 3, where the values of χ^2/dof characterizing the quality of fit are also shown. The extremely thin X-ray brightness profile observed in SN 1006 and in other young SNRs is a result of strong synchrotron losses due to the strongly amplified magnetic field value in these SNRs [17, 18, 19]. Since the absolute values of the experimental brightness profiles and the actual shock position are not known, their values were used as adjusting parameters in the fitting procedure. As can be seen from Fig. 3, the magnetic field value $B_0 = 20 \mu\text{G}$ slightly overestimates the profile width. Together with the spectral fit (Fig. 2) we conclude that $B_0 = 30 \mu\text{G}$ ($B_d \approx 150 \mu\text{G}$) is a realistic estimate.

Fig. 4 show the calculated integral γ -ray energy fluxes from the North-Eastern (NE) half of the remnant, in order to compare with the reported CANGAROO emission from the NE rim and the corresponding upper limit from H.E.S.S. These calculated fluxes correspond to 50 % of the entire theoretical γ -ray flux from SN 1006 under our assumption of dipolar symmetry [21].

The key point is that a decrease of the ISM density leads to a considerable reduction of the expected π^0 -decay γ -rays (see Fig. 4): in the Sedov phase the π^0 -decay γ -ray flux $F_\gamma^\pi \propto N_H E_c$ is proportional to the gas density and to the CR energy content E_c . This roughly implies $F_\gamma^\pi \propto N_H^2$ and is in agreement with the numerical results. The IC γ -ray flux is only weakly sensitive to the gas density as Fig. 4 also indicates. A modification of the magnetic field strength would not change much the π^0 -decay γ -ray flux, and thus the total γ -ray flux, whereas the IC flux decreases considerably with increasing magnetic field strength.

The non-detection of SN 1006 by the H.E.S.S. experiment [4] implies that the hydrogen density N_H is lower than 0.1 cm^{-3} , and excludes the high value $N_H = 0.3 \text{ cm}^{-3}$ which happened to fit the CANGAROO data. As

clearly shown in Fig. 4, at 1 TeV and for $B_0 = 30\mu\text{G}$, the H.E.S.S. upper limit is still about three times larger than the total γ -ray flux from SN 1006, expected for $N_H = 0.05\text{ cm}^{-3}$, which is at the lower end of the range $0.05 \leq N_H \leq 0.3\text{ cm}^{-3}$ of plausible ambient densities.

Since the IC γ -ray emission is quite insensitive to the ISM density, the *lower limit* for the expected γ -ray flux at TeV energies — in the form of the IC flux, derived from the integrated synchrotron flux and the field amplification alone — is about a factor of five lower than the H.E.S.S. upper limit. Such a low γ -ray flux from SN 1006 would be expected if the ambient ISM number density N_H was even considerably lower than 0.05 cm^{-3} .

We conclude from the above consideration that the H.E.S.S. upper limit does not invalidate the theoretical picture [3] on which the previous calculation of the γ -ray emission spectrum has been based. It is shown that the value of the external astronomical parameter N_H strongly influences the hadronic γ -ray flux. In the case of SN 1006, and in other similar cases, γ -ray detections will at the same time give a reliable estimate of the ambient ISM density.

Given the arguments above, it is certainly worth to attempt the detection of this important source in a deep observation of about 200h with the H.E.S.S. experiment.

This work has been supported in part by the Russian Foundation for Basic Research (grant 03-02-16524) and LSS 422.2003.2.

References

- [1] K. Koyama, R. Petre, E.V. Gotthelf et al., Nature 378, 255 (1995).
- [2] T. Tanimori, Y. Hayami, S. Kamei et al., ApJ 497, L25 (1998).
- [3] E.G. Berezhko, L.T. Ksenofontov, H.J. Völk, A&A 395, 943 (2002).
- [4] F.A. Aharonian, A.G. Akhperjanian, K.-M.H. Aye et al., astro-ph/0502239 (2005).
- [5] E.G. Berezhko, V.K. Elshin, L.T. Ksenofontov, JETP 82, 1 (1996).
- [6] E.G. Berezhko, H.J. Völk, Astropart. Phys. 7, 183 (1997).
- [7] V.V. Dwarkadas, R.A. Chevalier, ApJ 497, 807 (1998).
- [8] G.M. Dubner, E.B. Giacani, W.M. Goss et al., A&A 387, 1047 (2002).
- [9] P.F. Winkler, G. Gupta, K.S. Long, ApJ 585, 324 (2003).
- [10] D.A. Moffett, W.M. Goss, S.P. Reynolds, AJ 106 (1993). 1566
- [11] A.J.S. Hamilton, C.L. Sarazin, A.E. Szymkowiak, ApJ 300, 698 (1986).
- [12] G.E. Allen, E.V. Gotthelf, R. Petre, Proc. 26th ICRC, Salt Lake City, Vol.3, p.480 (1999).
- [13] S.P. Reynolds, ApJ 459, L13 (1996).
- [14] S.G. Lucek, A.R. Bell, MNRAS 314, 65 (2000).
- [15] E.G. Berezhko, G. Pühlhofer, H.J. Völk, A&A 400, 971 (2003).
- [16] A. Bamba, R. Yamazaki, M. Ueno, K. Koyama, ApJ 589, 827 (2003).
- [17] E.G. Berezhko, L.T. Ksenofontov, H.J. Völk, A&A 412, L11 (2003).
- [18] E.G. Berezhko, H.J. Völk, A&A 419, L27 (2004).
- [19] H.J. Völk, E.G. Berezhko, L.T. Ksenofontov, A&A 433, 229 (2005).
- [20] S. Hara, Doctoral Thesis, Tokyo Institute of Technology (2002).
- [21] H.J. Völk, E.G. Berezhko, L.T. Ksenofontov, A&A 409, 563 (2003).